Available online at www.sciencedirect.com

ScienceDirect

Procedia Structural Integrity 12 (2018) 173–182

Structural Integrity
Procedia

www.elsevier.com/locate/procedia

AIAS 2018 International Conference on Stress Analysis

Effects of environment and stress concentration factor on Ti-6Al-4V specimens subjected to quasi-static loading

S. Baragetti[a,b]*, E. Borzini[c], E.V. Arcieri[a,b]

[a]GITT – Centre on Innovation Management and Technology Transfer, University of Bergamo, Via Salvecchio 19, Bergamo 24129, Italy
[b]Department of Management, Information and Production Engineering, University of Bergamo, Viale Marconi 5, Dalmine 24044, Italy
[c]Machine Designer, Via Lagrange 26, Novara 28100, Italy

Abstract

The bimodal titanium alloy Ti-6Al-4V is a well-known high strength-to-mass ratio material in different engineering sectors. Furthermore, the rapid oxidation of the surface protects the base material from the interaction with a wide spectrum of corrosive environments. However, the presence of surface defects and the mechanical loading may compromise the effectiveness of the oxide film. Quasi-static loading tests were carried out on different smooth and notched Ti-6Al-4V specimens in order to analyze the role of environment and stress concentration factor.

© 2018 The Authors. Published by Elsevier B.V.
This is an open access article under the CC BY-NC-ND license (http://creativecommons.org/licenses/by-nc-nd/3.0/)
Peer-review under responsibility of the Scientific Committee of AIAS 2018 International Conference on Stress Analysis.

Keywords: Ti-6Al-4V, quasi-static loading test, notch sensitivity, aggressive environment

1. Introduction

As stated in Lutjering et al. (2007), Ti-6Al-4V is one of the most widespread high strength-to-mass ratio alloy in aerospace, automotive and marine advanced applications. Furthermore, Dimah et al. (2012) pointed out that this alloy is widespread in biomedical fields thanks to its biocompatibility and encouraging interaction with the body environment while Gurrappa (2003) underlined the high resistance to a huge spectrum of corrosive environments due

---

* Corresponding author. Tel.: +39-035-205-2382; fax: +39-035-205-2221.
E-mail address: sergio.baragetti@unibg.it

2452-3216 © 2018 The Authors. Published by Elsevier B.V.
This is an open access article under the CC BY-NC-ND license (http://creativecommons.org/licenses/by-nc-nd/3.0/)
Peer-review under responsibility of the Scientific Committee of AIAS 2018 International Conference on Stress Analysis.
10.1016/j.prostr.2018.11.097

to the quick formation of protective surface oxides. Unfortunately, the resistance to corrosion can decrease in presence of tensile and fatigue loads, as reported in Codaro (2003).

A long series of experimental tests were carried out in order to characterize the Ti-6Al-4V alloy and its behavior in different environments.

Morrisey et al. (2005) investigated the fatigue strength of Ti-6Al-4V at 60 Hz and 20kHz finding out no frequency effects while Lanning et al. (2005) tested smooth and notched specimens with different stress concentration factors in order to evaluate the maximum stress for 1,000,000 cycles. Bellows et al. (1999) validated the step test method for Ti-6Al-4V specimens. Leuders et al. (2013) highlighted the detrimental effects of the porosity on fatigue strength of additive manufactured Ti-6Al-4V specimens. Van Hooreweder et al. (2012) investigated the fatigue strength of Selective laser melting (SLM) and find out a reduction of the fatigue strength of SLM Ti-6Al-4V. Since an equal density of the SLM Ti-6Al-4V and conventionally produced specimens was imposed, Van Hooreweder et al. (2012) concluded that the lower fatigue properties are most likely due to the anisotropy of the microstructure. Seifi et al. (2017) studied specimens processed by electron beam melting (EBM) concluding that in general their fatigue behavior was similar to the cast and wrought Ti-6Al-4V.

Nalla et al. (2002) studied a fine-grained equiaxed bimodal and a coarser lamellar microstructure in order to evaluate the effects on mixed mode high-cycle fatigue behavior pointing out that lamellar microstructure is characterized by higher thresholds.

Different environments were also investigated. For example, Sanderson et al. (1968) tested U-specimens and found out that Ti-6Al-4V is not susceptible to Stress Corrosion Cracking (SCC) in seawater. In a similar work described in Sanderson et al. (1968), a significant SCC sensitivity was noticed for Ti-6Al-4V alloy in pure methanol and methanol-HCl solutions. The effects of the methanol on Ti-6Al-4V pressurized fuel tanks was observed also in Johnston et al. (1967) and Johnson et al. (1967) for static and fatigue loading. Johnston et al. (1967) however pointed out that only 1% of moisture or cathodic protection are sufficient to inhibit SCC.

In view of that, the Structural Mechanics Laboratory (SM-Lab) research group of the University of Bergamo is carrying out a Stress Corrosion Cracking (SCC) and Corrosion Fatigue (CF) experimental campaign in air, sea water (3.5% wt. NaCl) and different methanol concentrations. These experiments are described in Baragetti et al. (2013), Baragetti et al. (2013), Baragetti et al. (2014), Baragetti et al. (2014), Baragetti et al. (2015), Baragetti et al. (2015), Baragetti et al. (2016) and summarized in Baragetti et al. (2018). The research topic is the investigation of the effect of the environment on various loading conditions, in terms of fatigue strength, with the separation of the chemical and mechanical driving forces involved in fatigue phenomena.

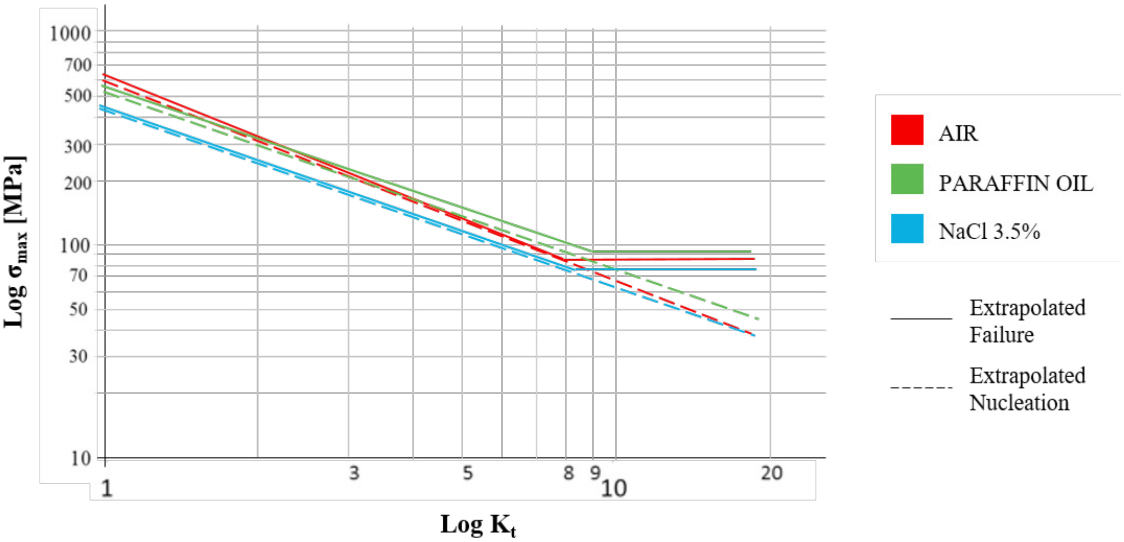

Fig. 1. Maximum stress vs stress concentration factor, fatigue loading, adapted from Baragetti et al. (2018).

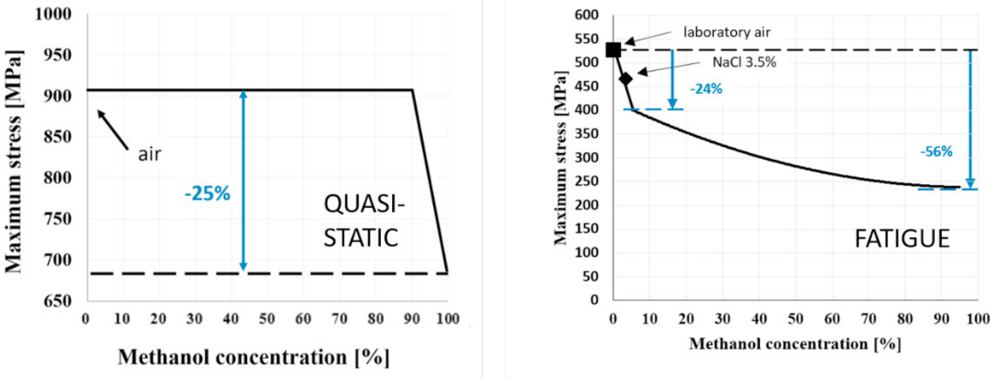

Fig. 2. Maximum stress vs methanol concentration, quasi-static and fatigue loading, adapted from Baragetti et al. (2018).

The outcomes of these experiments pointed out the presence of a threshold for maximum stress (K_t=8-9, Fig. 1) for Ti-6Al-4V under cyclic loading. These results are in accordance with Frost and Dugdale (1957) for mild steel even if the threshold value for the stress concentration factor is 3-4. The reason of this difference can be the higher propagation rate for Ti-6Al-4V as stated in Baragetti et al. (2015). In Baragetti et al. (2018) can be also seen the effects of methanol solutions on the quasi-static and fatigue strength of the alloy: only methanol concentrations higher than 90% wt. are detrimental for quasi-static loading (-25% for pure methanol), while also small concentrations are detrimental for fatigue loading (-24% for 15% wt. methanol and -56% for pure methanol, Fig. 2).

In this paper quasi-static tests on Ti-6Al-4V, not STOA (Solution Treatment and Over-Aging) treated, specimens are described. STOA treatment consists of a 1 h solution treatment (925°C) and following over-aging carried out by means of a 2 h vacuum annealing (700°C), as stated in Baragetti et al. (2018). The specimens were smooth and notched and were tested in inert environment (air and paraffin oil) and aggressive environment (methanol solution).

Nomenclature

A%	elongation
E	Young modulus
K_t	stress concentration factor
r	radius of the notch
UTS	ultimate tensile strength
YS	yield strength

2. Experimental tests

The specimens were obtained from a Ti-6Al-4V raw plate supply and were not subjected to STOA treatment. The mechanical properties of the specimens are reported in Table 1.

Table 1. Mechanical properties.

UTS [MPa]	YS [MPa]	E [MPa]	A%
1,000-1,100	958-1,050	110,000	16

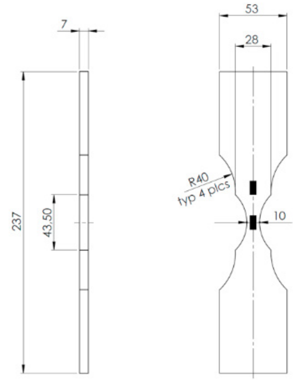

Fig. 3. Smooth specimen.

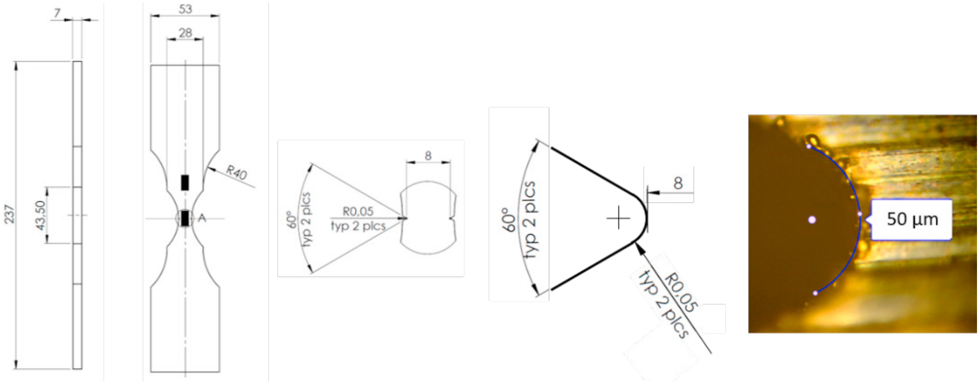

Fig. 4. EDM notched specimen.

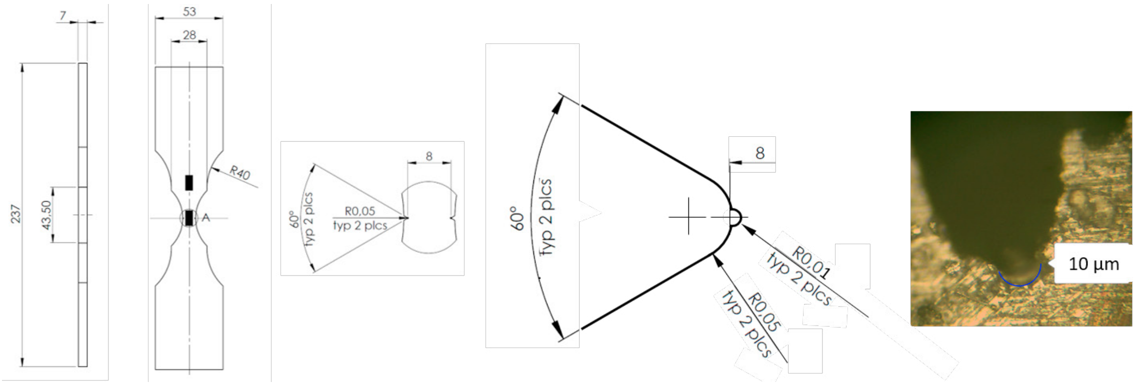

Fig. 5. EDM+sharp knife notched specimen.

Three different shapes were tested. In this paper, they are called “smooth specimen”, “EDM notched specimen” and “EDM+sharp knife notched specimen” (Fig. 3, Fig. 4 and Fig. 5). For the EDM notched specimen, two notches (one left and one right) were carried out by means of Electro Discharge Machining (EDM) and can be seen in Fig. 4. For the EDM+sharp knife notched specimen, two further notches (one left and one right) were carried out by means of a sharp knife on the previous EDM notches (Fig. 5). In Fig. 3 and Fig. 4, the positioning of the strain gauges can be seen (two on the front side, two on the rear side). The strain gauges in the central zone were not placed during the tests in aggressive environments in order to avoid contamination. In this way, the stress on the specimen can be monitored during the setup and the test (a load cell was also used during the test).

The local stress concentration factors for the three geometries were calculated by means of linear elastic finite element modelling with plane-stress elements and are reported in Table 2. For the calculation the maximum principal stress was used.

Table 2. Stress concentration factors.

	K_t
Smooth specimen	1.1
EDM notched specimen	8.1
EDM+sharp knife notched specimen	18.0

The specimens were loaded by means of a testing machine (Fig. 6) specifically designed by the SMLab research group. The machine consists of a threaded road tensile system and rolling bearing hinge grips to avoid parasite bending moments. The plate behind the two grips is useful during the setup of the test in order to avoid bending stress on the specimen.

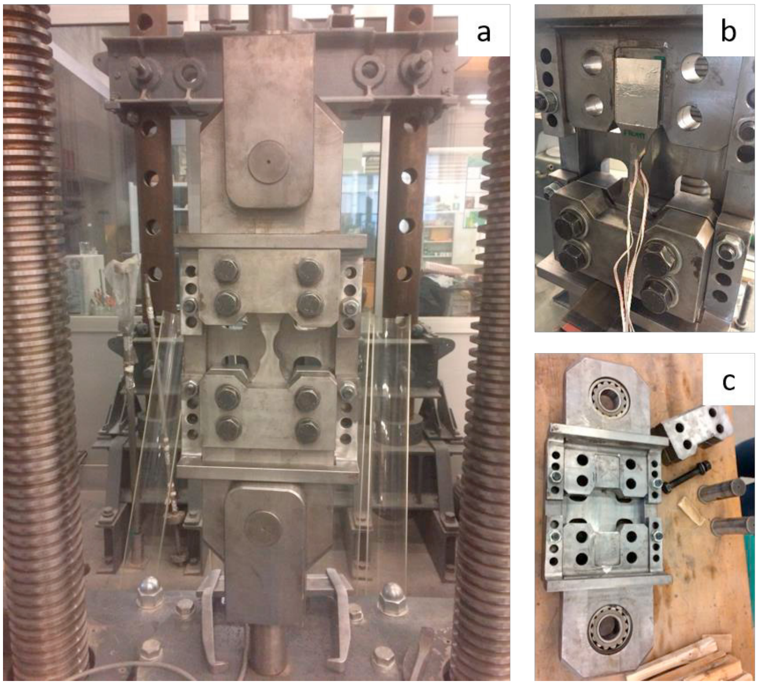

Fig. 6. Testing machine: (a) general view; (b), (c) details.

After the polishing of the specimens by means of grinding papers and diamond paste, abrasive blasting operations on the gripping points were carried out in order to reach more friction. Aluminum tape pieces were placed so that they work like a gasket and they inhibit the sliding of the specimen in the machine (Fig. 7).

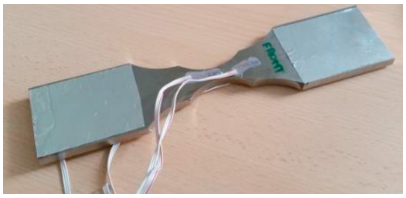

Fig. 7. Preparation of the specimen.

2.1. Smooth specimen in inert environment (air)

The first test was carried out on a smooth specimen in inert environment (air). The stress in Fig. 8 was applied on the specimen. In Fig. 8, also the strain rate is plotted. All the tests were carried out at low strain rates.

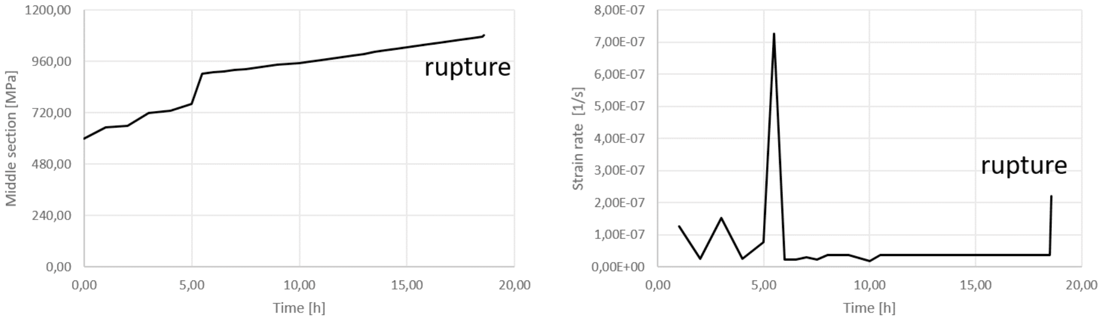

Fig. 8. Smooth specimen in inert environment (air): stress in the middle section and strain rate.

2.2. EDM notched specimen in inert environment (paraffin oil)

This test (Fig. 9) was carried out in order to evaluate the effects of the EDM notch. Paraffin oil was used in order to simulate vacuum conditions.

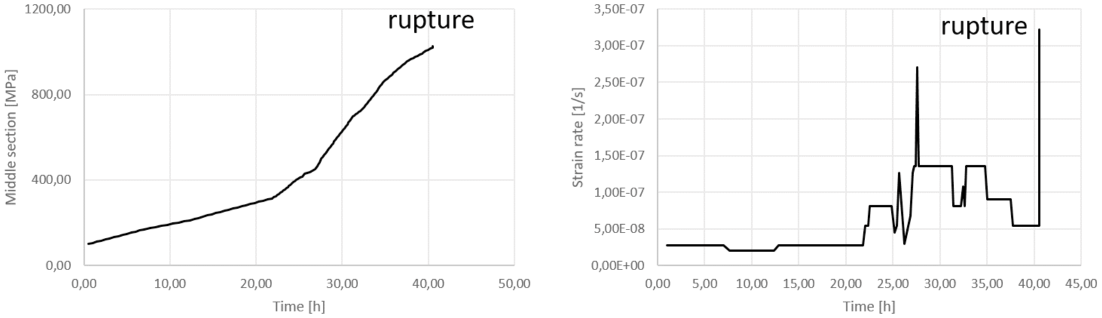

Fig. 9. EDM notched specimen in inert environment (paraffin oil): stress in the middle section and strain rate.

2.3. EDM notched specimen in pure methanol

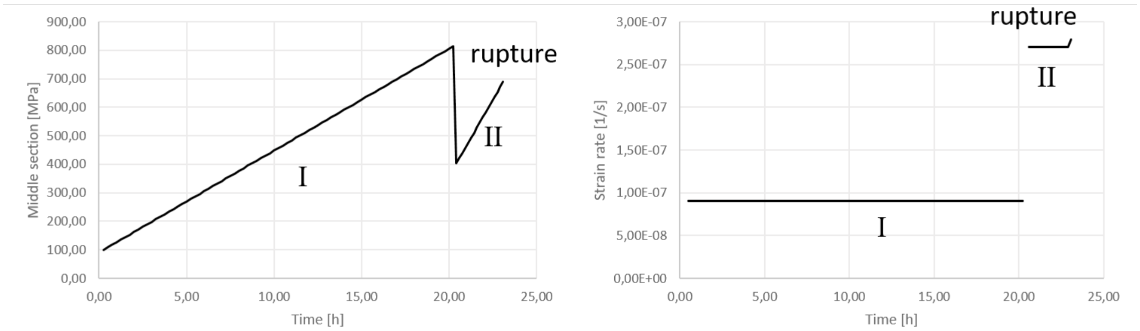

Fig. 10. EDM notched specimen in pure methanol: stress in the middle section and strain rate.

The load history and the strain rate for this test are reported in Fig. 10. This test consists of two phases. During the first phase the methanol was contained in a tank made of two PVC pieces connected by means of silicone (Fig. 11a). A stress higher than 800 MPa was reached without failure and the contamination of the methanol with silicone was noticed. Because of the idea of a possible reduced effectiveness of the methanol due to this contamination, a different tank was adopted. Here the two PVC pieces were linked by means of bolts and another type of sealant unable to react with methanol (Fig. 11b).

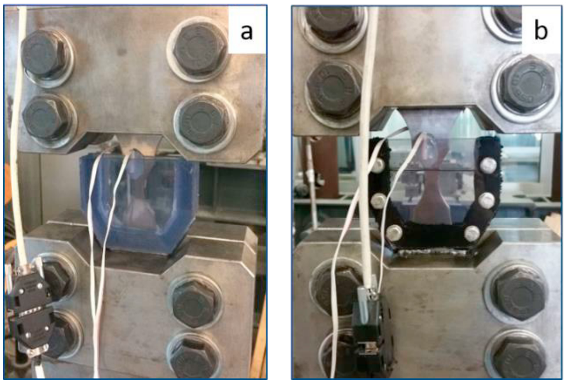

Fig. 11. Tank for the containment of the methanol, (a) first version, I phase, (b) second version, II phase.

Methanol was added during the test and removed whenever the test was paused in order not to accelerate the corrosion phenomena.

2.4. Smooth specimen in pure methanol

Fig. 12 summarizes the imposed load and strain rate. Methanol was added during the test and not removed during the stops. During the stops a small load was applied.

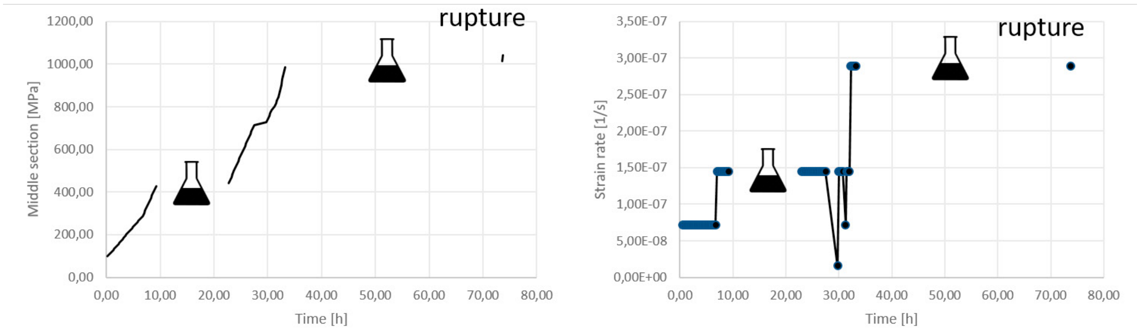

Fig. 12. Smooth specimen in pure methanol: stress in the middle section and strain rate.

2.5. EDM+sharp knife notched specimen in pure methanol

For this test, a completely sealed tank was used. The tank was also completely filled with methanol so that moisture cannot penetrate and contaminate the solution. It has to be reminded indeed that moisture can reduce the effectiveness of the methanol, as stated in Johnston et al. (1967).

Fig. 13 summarizes the load steps adopted. The last step was 345 MPa and was set to take 1 hour. However, after this time, the load on the specimen was 0 MPa and when an increment of load was attempted, the failure occurred.

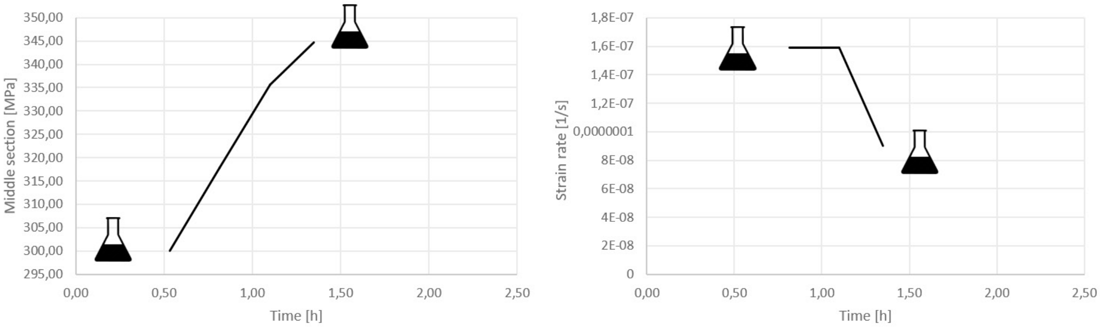

Fig. 13. EDM+sharp knife specimen in pure methanol: stress in the middle section and strain rate.

3. Results and discussion

Fig. 14 summarizes the outcomes of the described tests in terms of stress and time to failure. It could be stated that no significant differences appeared for specimens in inert environment, K_t =1.1 and 8.1. At the same time methanol has no effects on smooth specimen if Ti-6Al-4V is not subjected to STOA treatment while an appreciable reduction was observed in Baragetti et al. (2018) for the treated specimen. No appreciable differences between STOA K_t=1.18 and not STOA treated K_t=8.1 specimens can be noticed while a drastic reduction of maximum stress was observed for K_t=18 in pure methanol.

The rupture occurred in a brittle way for all the specimens, except the EDM+sharp knife notched specimen.

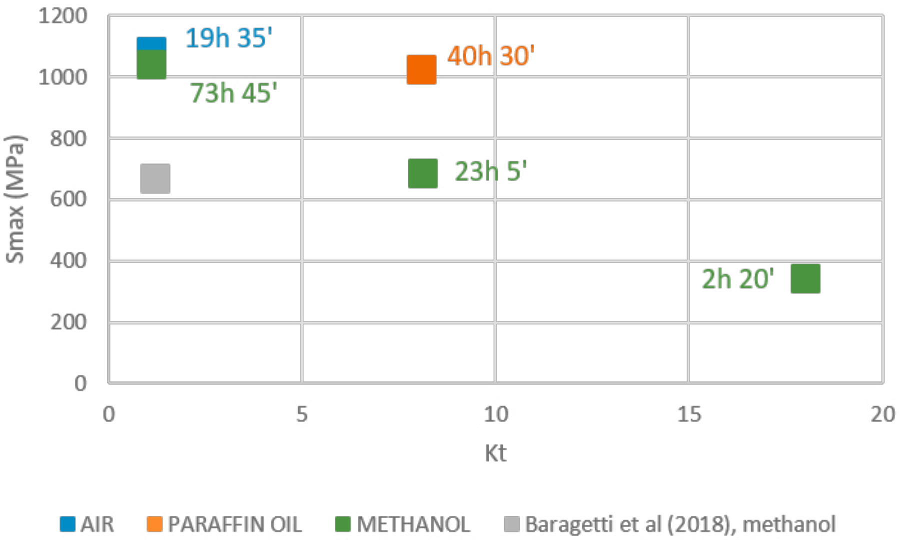

Fig. 14. Results.

During the analysis of the results, some important aspects have to be taken into account. First of all, the tests were not carried out at the same strain rate so the specimens were in contact with methanol for different times. Furthermore, the methanol used during the third and fourth test could have been contaminated by the moisture in air because the tank was not completely sealed. A chemical analysis of the methanol after the test could be necessary in order to verify an eventual contamination of the methanol solution. An example of the effects of the possible combination of these two factors is the third test: at the end of the first phase a load higher than 800 MPa was reached but some modifications of the test parameters were sufficient to have a stress to failure of about 700 MPa.

4. Conclusions

Quasi-static loading tests were performed on smooth and notched specimens in different environments in order to characterize the behavior of Ti-6Al-4V, not STOA treated. In particular, three different stress concentration factors (K_t=1.1, 8.1 and 18) and three different environments were investigated (inert environment: air and paraffin oil, aggressive environment: pure methanol).

The results highlighted no notch sensitivity for specimens in inert environments, for K_t=1.1 and 8.1. Also the methanol seems to be not effective on smooth specimens. For methanol, K_t=8.1, a stress to failure equal to the maximum stress for STOA treated K_t=1.18 specimens, shown in Baragetti et al. (2018), was reached.

Only pure methanol, without contamination with moisture and air, seems to have detrimental effects.

Further studies are mandatory in order to verify the results here presented and to investigate other stress concentration factor – environment combinations. An analysis of the methanol solutions after the test could be interesting in order to verify the composition of the solution and the presence of other chemical species in the solution.

Acknowledgements

The authors wish to thank Giorgia Casappa, Loris D'Ettore and Federico Giuseppe for their contribution to the research activity.

References

Baragetti, S., Foglia, C., Gerosa, R., 2013. Fatigue Crack Nucleation and Growth Mechanisms for Ti-6Al-4V in Different Environments. Key Engineering Materials 525-526, 505-508.

Baragetti, S., Medolago, A., 2013. Load and environmental effects on the corrosion behavior of a Ti-6Al-4V. Key Engineering Materials 525-526, 501-504.

Baragetti, S., 2014. Notch Corrosion Fatigue Behavior of Ti-6Al-4V. Materials 7 (6), 4349-4366.

Baragetti, S., Villa, F., 2014. SCC and corrosion fatigue characterization of a Ti-6Al-4V alloy in a corrosive environment – experiments and numerical models. Frattura ed Integrità Strutturale 8(30), 84–94.

Baragetti, S., Villa, F., 2015. Corrosion Fatigue of High-Strength Titanium Alloys Under Different Stress Gradients. The Journal of the Minerals, Metals & Materials Society (JOM) 20 67(5), 1154-1161.

Baragetti, S., Villa, F., 2015. Quasi-Static Behavior of Notched Ti-6Al-4V Specimens in Water-Methanol Solution. Corrosion Reviews 33(6), 477-485.

Baragetti, S., Villa, F., 2016. Crack propagation models: numerical and experimental results on Ti–6Al–4V notched specimens. Fatigue & Fracture of Engineering Materials & Structures 40(8), 1276-1283.

Baragetti, S., Arcieri, E.V., 2018. Corrosion fatigue behavior of Ti-6Al-4V: Chemical and mechanical driving forces. International Journal of Fatigue 11, 301-307.

Bellows, R.S., Muju, S., Nicholas, T., 1999. Validation of the step test method for generating Haigh diagrams for Ti-6Al-4V. International Journal of Fatigue 21(1), 687-697

Codaro, E.N., Nakazato, R.Z, Horovistiz, A.L., Ribeiro, L.M.F., Ribeiro, R.B., Hein, L.R.O., 2003. An image analysis study of pit formation on Ti-6Al-4V, Materials Science and Engineering A 341, 202–210.

Dimah, M.K., Devesa Albeza, F., Amigó Borrás, V., Igual Muñoz, A., 2012. Study of the biotribocorrosion behavior of titanium biomedical alloys in simulated body fluids by electrochemical techniques, Wear, 294–295, 409–418.

Frost, N.E., Dugdale, D.S., 1957. Fatigue tests on notched mild steel plates with measurements of fatigue cracks. Journal of the Mechanics and Physics of Solids 5(3), 182-192

Gurrappa, I., 2003. Characterization of titanium alloy Ti-6Al-4V for chemical, marine and industrial applications. Materials Characterization 51, 131– 139

Johnson, R.E., 1967. Nasa Experiences with- Ti-6al-4V in Methanol, DMIC Memorandum 228, 2–7.

Johnston, R.L., Johnson, R.E., Ecord, G.M., Castner, W.L., 1967. Stress-Corrosion Cracking of Ti-6al-4V Alloy in Methanol, NASA Technical Note TN D-3868.

Lanning, D.B., Nicholas, T., Haritos, G.K., 2005. On the use of critical distance theories for the prediction of the high cycle fatigue limit stress in notched Ti–6Al–4V. International Journal of Fatigue 27, 45-57.

Leuders, S., Thöne, M., Riemer, A., Niendorf, T., Tröster, T., Richard, H., Maierad, H., 2013. On the mechanical behaviour of titanium alloy Ti6Al4V manufactured by selective laser melting: Fatigue resistance and crack growth performance. International Journal of Fatigue 48, 300-307.

Lütjering, G., Williams, J.C., 2007. Titanium, second edition, Springer, Berlin.

Morrissey, R.J, Nicholas, T., 2005. Fatigue strength of Ti–6Al–4V at very long lives. International Journal of Fatigue 27(10-12),1608-1612.

Nalla, R.K., Campbell, J.P., Ritchie, R.O., 2002. Effects of microstructure on mixed-mode, high-cycle fatigue crack-growth thresholds in Ti-6Al-4V alloy. Fatigue & Fracture of Engineering Materials & Structures 25(6), 587-606.

Sanderson, G., Powell, D.T., Scully, J.C., 1968. The Stress-Corrosion Cracking of Ti Alloys in Aqueous Chloride Solutions at Room Temperature. Corrosion Science 8, 473–481.

Sanderson, G., Scully, J.C., 1968. The Stress-Corrosion Cracking if Ti Alloys in Methanolic Solutions. Corrosion Science 8, 541–548.

Seifi, M., Salem, A., Satko, D., Shaffer, J., Lewandowsk J.J., 2017. Defect distribution and microstructure heterogeneity effects on fracture resistance and fatigue behavior of EBM Ti–6Al–4V. International Journal of Fatigue 94, 263-287.

Van Hooreweder, B., Boonen, R., Moens, D., Kruth, J.P., Sas, P., 2012. On the determination of fatigue properties of Ti-6Al-4V produced by selective laser melting, Collection of Technical Papers - AIAA/ASME/ASCE/AHS/ASC Structures, Structural Dynamics and Materials Conference.